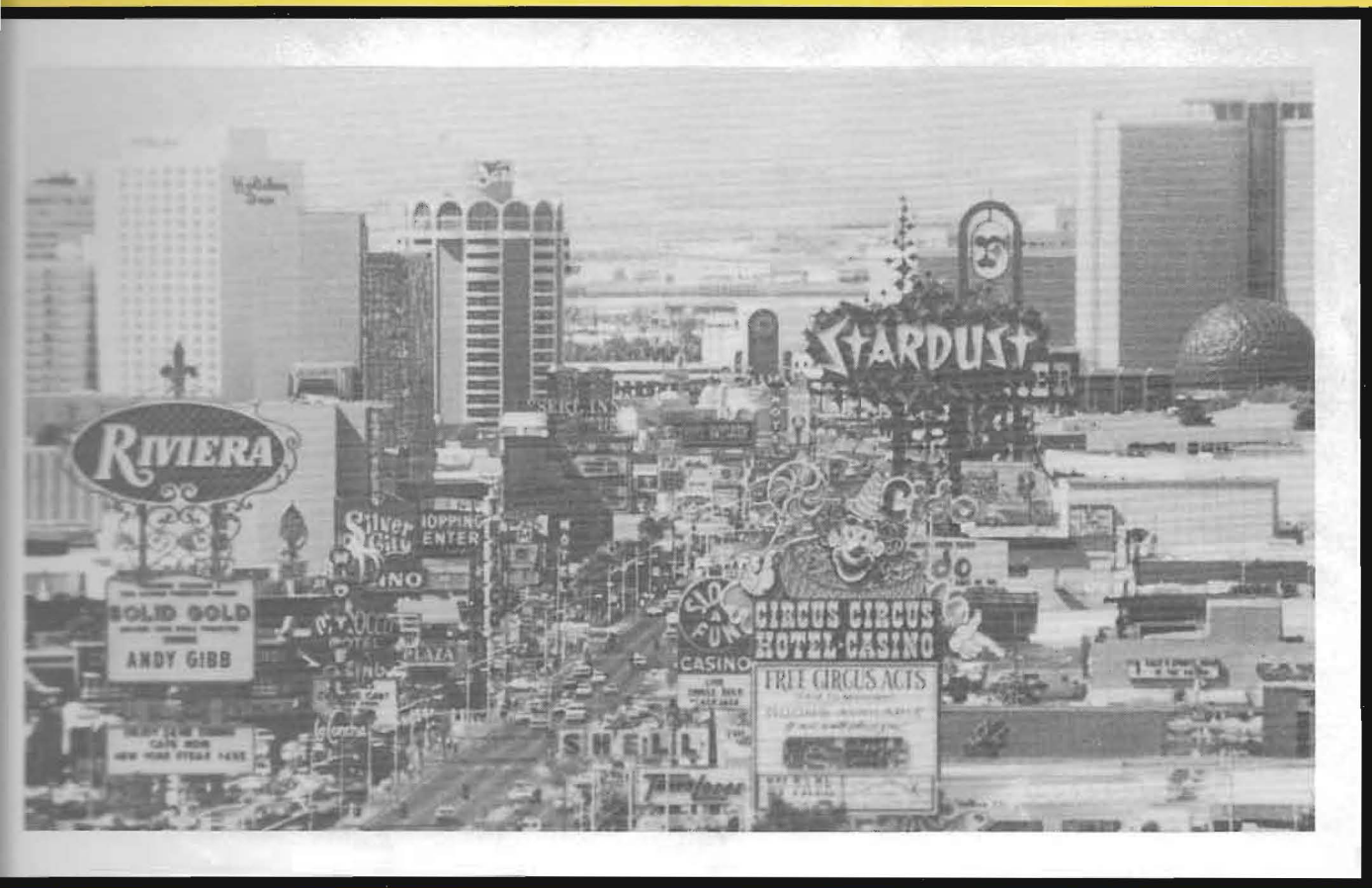


G. O. Z

Bulletin of the American Physical Society

Program of the March Meeting of The American Physical Society:
March - 4 April 1986, Las Vegas, Nevada



creasing temperature down to 0.35 K. Since thermal-broadening effects are negligible in comparison to collision-broadening of the Landau levels at these temperatures, our data are not consistent with models^{1,2} that attribute the negative magnetoresistance to Landau levels in a quasi-two-dimensional band structure. Implications regarding the morphology of these fibers and its effects on their applications will be discussed.

*Supported by NASA, Grant # NCC-3-19.

†Supported by the NSF Low-Temperature Physics Program, Grant # DMR-8204173.

1 A. A. Bright, Phys. Rev. B20, 5142 (1979).

2 K. Yazawa, J. Phys. Soc. Japan 26, 1407 (1969).

well PR 330 801 (1984)

10:48

MP 10 X-Ray Determination of the Substrate Modulation Potential for a 2-D Rb Liquid in Graphite. S.C. MOSS, G. REITER, J.L. ROBERTSON, C. THOMPSON, University of Houston; K. OHSHIMA, Nagoya University.-- Using a recent theory¹ for the scattering of X-rays by 2-D liquids in a periodic host, we have determined the Fourier coefficients, V_{HK} , of the graphite modulation potential $V(r)$, for a Rb liquid intercalated to stage 2 in graphite. Apart from the effects on the liquid scattering pattern, this induced potential produces contributions of Rb to the (HK.L) graphite Bragg peaks and these may be used to compute V_{HK} via a Monte Carlo (iterative) procedure. The dominant contribution turns out to arise from the first term, V_{10} , which is about -0.01eV.

* Research supported by NSF: DMR-82-14314

1. George Reiter and S.C. Moss (submitted to Phys. Rev.)

11:00

MP 11 Magnetoresistivity and Monte Carlo Studies of Magnetic Phase Transitions in C_6Eu .† S.T. CHEN, G. DRESSELHAUS, M.S. DRESSELHAUS; MIT, H. SUEMATSU, H. MINEMOTO, K. OHMATSU; Tsukuba Univ., AND Y. YOSIDA; Toyama Univ.--The high field magnetoresistivity $\rho(H)$ of the antiferromagnetic first stage graphite intercalation compound C_6Eu has been measured in steady magnetic fields up to 28 T with $\vec{H} \perp \vec{c}$ and $\vec{H} \parallel \vec{c}$. Both longitudinal ($\vec{J} \parallel \vec{H}$) magnetoresistivity $\rho_L(H_{\parallel})$ and transverse ($\vec{J} \perp \vec{H}$) magnetoresistivity $\rho_T(H_{\perp})$ with $\vec{H} \perp \vec{c}$ show distinct changes across the magnetic phase boundaries which occur at fields of 1.5T, 8T, 15T and 21.5T at a temperature of 4.2 K. The phase transition at $H=15T$ was not observed previously by the pulsed magnetization measurements. A Monte Carlo simulation based on the Hamiltonian of Sakakibara and Date was carried out for the C_6Eu system. The 15T phase transition is explained as a transition from a "canted" to a "fan" state. The transverse magnetoresistivity $\rho_T(H_{\parallel})$ with $\vec{H} \parallel \vec{c}$ shows a clear anomaly at the field corresponding to the onset of the transition to the spin aligned paramagnetic state. A magnetic phase diagram has been accurately determined based on the results of the magnetoresistivity measurements. The various spin configurations in the phase diagram are identified and the parameters of the Hamiltonian determined using the results of the Monte Carlo simulation.

†Work at MIT supported by AFOSR Contract #F49620-83-C-0011.

11:12

MP 12 Photoconductivity of Graphite Fibers.† J. STEINBECK, G. BRAUNSTEIN, F. YU, M.S. DRESSELHAUS, MIT, T. VENKATESAN, Bell Comm. Res.--A photoelectric response has been observed in graphite fibers. The existence of a photoelectric response in graphite fibers is surprising since single crystal graphite is a semimetal. The rise and fall times of the photoelectric response have been measured to be on the order of 3ms, suggesting a trapping mechanism for the observed photoelectric effect. Results for the dependence of the photoelectric response on temperature, fiber diameter, and heat treatment temperature are reported for temperatures ranging from 10K to 300K, diameters ranging from $5\mu m$ to $50\mu m$ and heat treatment temperatures up to 3300K. Our results suggest that the photoelectric response of graphite fibers is due to a trapping mechanism, consistent with the observed decrease in the photoelectric response signal below $\sim 170K$. The defect trapping mechanism also explains the decrease in photoelectric response as the fiber diameter is increased, and as the heat treatment temperature is increased. The observation of a photoelectric response may provide a new technique for studying defects in graphite. In this regard it is significant that highly oriented pyrolytic

graphite (HOPG) shows no photoelectric response. The effect of intercalation on the photoelectric response will be discussed.

†The MIT authors acknowledge support from AFOSR Contract #F49620-85-C0147.

11:24

MP 13

c-axis Resistivity of $FeCl_3$ Intercalated Graphite *

A. Ibrahim, R. Powers, M. Tahar and G.O. Zimmerman, Boston University.

The c-axis resistivity of stage 2, 3, 4, 5 and 9 of $FeCl_3$ intercalated graphite, as well as that of HOPG was measured by means of a four terminal method between room temperature and 1K. The room temperature resistivities are 1.15, 1.08, 0.784, 1.63, 0.701 and 0.098 for stage 2, 3, 4, 5, 9 and HOPG respectively. The temperature coefficient of the resistivity is negative in stages 2, 3 and 4, approximately zero in stage 5, and positive in stage 9 and HOPG. The data are in qualitative agreement with the theory of Sugihara¹.

* Supported by the Air Force Office of Scientific Research Grant AFOSR 82-0286.

1) K. Sugihara, Phys. Rev. 29B, 5872, (1984).

Supplementary Program

MP 14

Spin Lattice Relaxation in Stage-6 $FeCl_3$ Intercalated Graphite Near the 1.75K Magnetic Anomaly.

A. Ibrahim and G.O. Zimmerman, Boston University.

The relaxation time of Fe^{3+} ions in stage-6 intercalated graphite was measured by means of the Casimir & du Pre method¹ in the vicinity of the 1.75K magnetic anomaly². The in and out of phase susceptibility was measured at frequencies of 40, 100, 400, 800, and 1000 Hz. It is found that there is a maximum in the relaxation time near the anomaly and that there the ratio of the specific heats at constant field to that at constant magnetization also has a maximum. The two maxima are displaced in temperature.

* Supported by the Air Force Office of Scientific Research Grant AFOSR 82-0286.

1) Casimir & du Pre, Physica 5 507 (1938).

2) Zimmerman, Nicolini, Solenberger and Gata, p.101 Extended Abstracts, Proceedings of Symposium 1, 1984 Fall Meeting of the Materials Research Society, Eklund, Dresselhaus and Dresselhaus editors. MRS Pittsburgh, 1984.

MP 15 Localized Phonons in Stage Disordered Graphite Intercalation Compounds. P. HAWRYLAK

and M. L. WILLIAMS, Brown University.*-- The effect of stage disorder(1,2) on [001]L phonons in intercalated graphite is studied. The energies and localization length of phonons associated with stage 3 and 5 impurity units in stage 4 potassium-graphite are calculated. The phonon density of states is predicted as a function of stage disorder and compared with random distribution of potassium in the graphite host.

* Supported in part by the U. S. Army Research Office, Durham.

1. G. Kirczenow, Phys. Rev. Lett. 52, 437 (1984)

2. M. E. Meisenheimer and H. Zabel, Phys. Rev. Lett. 54, 2521 (1985).

Williams, Ellen D. — EK2, EK10, EK12
Williams, G.A. — JM4
Williams, G.P. — KI15
Williams, G.P., Jr. — NU14
Williams, Jack M. — HO3, HO4
Williams, J.M. — DO12, HO1, HO2, HO5, HO7
Williams, M.L. — MP15
Williams, M.W. — EP10
Williams, R.S. — DJ10
Williams, R.T. — NU14
Williams, Wayner S. — DX3, Hwa34
Williams, W.S. — BP11, MG8, MG9, MH10
Williamson, D.L. — JN14
Williamson, S.J. — BP10
Willis, C. — HK10
Willis, J.O. — DR19, GR1, GR7, GR10, MR6
Wills, J.M. — ER9
Wilsey, N.D. — HT11, HT14
Wilson, B.A. — JT1
Wilson, J.C. — KX1
Wilson, K.G. — AM4
Wilson, L. — MG5
Wilson, Lane — KG6
Wilson, R.J. — AJ11, NV8
Wilson, T.M. — EV4, JG6
Wiltzius, P. — HI5
Wimberly, B.T. — DP8
Wimmer, E. — BJ2
Wind, S. — KO1
Wingreen, N.S. — BS5
Winokur, M. — AL6
Winokur, M.J. — KP16
Winter, H.H. — GwB14
Winter, J.J. — JT14
Wintersgill, M.C. — KW2
Wise, P. — JV4
Witowski, A. — EU2
Witt, S.N. — MS9
Witten, T.A. — HI8
Wittlin, A. — EU2
Woicik, J. — EI6
Wolf, Edward D. — CA1
Wolf, E.L. — GO4, MR1, MR2
Wolf, S.A. — DI2, DO5, DO8, NV14
Wolfe, J. — DP16
Wolfe, J.P. — DU2, DU4
Wolff, W.F. — EF7
Wolford, D.J. — JT6
Wolford, Donald J. — BT1
Won, H. — AR13
Wong, C.K. — AN14, GI1
Wong, E. — GR15
Wong, G. — HN2
Wong, G.K. — BS9
Wong, K.M. — BG11, BG12, BG13
Wong, K.Y.M. — DM2
Wong, S. — AU8
Woo, K.C. — DS10, MT7
Wood, D.M. — BU17, ET5
Woodall, J.M. — AS2, NH10
Woods, S.B. — JO5
Woodward, A.E. — AW8
Woodyard, J.R. — AI2
Wool, R.P. — AX10, BW8, BX2, DX10
Woolam, J.A. — MU2
Woollam, J.A. — NV11
Woollam, John A. — HN7, HN8, MP5, MP6
Worlock, J.M. — DT4, JT15, KL3
Woronick, S.C. — ET8, MS14
Worrell, G.A. — EY28
Worthington, M. — DJ5
Wortman, Deborah — JH6
Woyanovich, F. — GL6
Wright, D.C. — GG11
Wright, N.F. — AW12
Wright, S. — BS1, BS2, KT5
Wright, S.L. — HT1
Wroge, M.L. — MT5
Wronski, C.R. — DN1
Wu, C. — HWb6
Wu, C.Z. — MO5
Wu, G.-L. — Gwa8
Wu, G.Y. — MT12
Wu, Ji-Wei — JS6
Wu, J.-W. — JS10, KS6
Wu, J.Z. — HS7
Wu, M.K. — MR15
Wu, N.J. — DQ11
Wu, P.K. — EK7
Wu, S. — MO5
Wu, S.C. — DJ9, NG8
Wu, Shi-Yu — NM7
Wu, S.Y. — NE2
Wu, Wen-Li — JX12
Wu, W.-K. — DL13
Wu, W.L. — JX13, JX14
Wu, Xiao-Lun — BL4, BL5
Wu, Y. — AG7
Wu, Z.-Q. — Hwa15
Wudl, F. — KI1, KI4, KI5, KI17
Wunder, S.L. — EX3
Wunderlich, B. — HwB34, JW7, JW15
Wyder, P. — KO16
Wylie, J.M. — HU8
Wysyn, G.M. — GL10, GL12, GL15, HL14
Wyzgoski, M.G. — DX1, Hwa33
Xammar Oro, Juan R. — JP10
Xia, K.-Q. — GQ10
Xia, S. — EV16
Xia, W. — NF2
Xiao, Gang — NF9
Xiaoguang, Wu — JS4, JS11
Xide, Xie — EK4
Xie, A. — BP1
Xie, K. — BN6, HN7
Xie, X.-C. — BL3
Xu, J. — AW8
Xu, J.H. — EV15
Xu, Y. — EX12
Xue, J. — KQ12, KQ13
Yablonovitch, E. — KJ13, KS15
Yafet, Y. — GL8
Yagi, T. — KR10
Yalisove, S.M. — DJ6, DJ13, DJ14
Yan, X. — BG5, HO9
Yan, Y.-X. — JQ1
Yandrofski, R. — BK10
Yang, Arnold C.M. — HwB5
Yang, C.H. — BS6
Yang, C.P. — JP12
Yang, C.Y. — EN2, KN6
Yang, D.P. — BG10
Yang, Gui-Lin — BT4
Yang, H. — JX13, MH12
Yang, H.D. — MO7, MR2
Yang, K.N. — GP5, MR13
Yang, L. — DN7, DN8
Yang, M. — NP14, NP15
Yang, P. — HWb6
Yang, P.-Y. — Hwa15
Yang, S.-R. Eric — GT12
Yang, W.P. — HwB28
Yang, X.Q. — AL17
Yang, Y. — NU13
Yao, H.D. — BI10, BI11
Yaracs, Richard — BP14, BP17
Yarmoff, J. — JI11
Yashima, H. — KI4
Yau, C. — HWb24
Ye, Y.-Y. — NI8
Yee, A.F. — Gwa13
Yee, K. — JF2
Yeh, H.L. — JK3
Yeh, J.J. — AJ12
Yeh, X.L. — BH2
Yeh, Y. — JP15
Yehia, Sherif — JV12
Yelon, W.B. — AP4
Yelon, William — HU3, HV9
Yen, M.Y. — JI4
Yen, W.M. — AQ9, KH8
Yeo, Y.K. — MS13, NS15
Yin, L. — KQ9
Ying, S.C. — BJ11, DQ8, HJ10, KK4
Yodershort, D. — EU3
Yokoi, C.S.O. — HL12
Yoon, Y.S. — AT15
York, B.R. — DF13
Yoshizumi, Shozo — NL1
Yosida, Y. — MP11
You, H. — EL12, MJ9
Young, A.P. — EM12, EM13, EM19
Young, D. — BK11
Young, R.T. — AI2
Youngdale, E.R. — NT4
Youngquist, S.E. — HG3
Ytterboe, S.N. — BM2, BM7, BS3
Yu, C.C. — AK13, MN16
Yu, F. — MP12
Yu, H.-S. — BX3
Yu, J.J. — BV7
Yu, L.S. — HH3
Yu, P.W. — AT10, GT4, GT6, MU3
Yu, P.Y. — BK8, EU12, HI16, MO3
Yu, R.Q. — DK4
Yu, W.C. — AX9
Yu, X. — KX9
Yu, Z.H. — NV6
Yue, Kwok To — EP9
Yuh, H.-J. — EN6
Zaanan, J. — HR7
Zabel, H. — AF2, BH17, HG3, JI8, KP4, KP5, KP6, KP7, KP15, MP2, NP9
Zach, R. — AP5
Zacher, R. — NF12
Zacher, R.A. — DL9
Zafraan, Jacob — GwB10
Zakaria, A. — BH7
Zaleski, H. — MP7
Zallen, R. — HH5, HH6
Zaluzec, N.J. — HN14
Zamani, N. — EI2
Zangwill, A. — AF3
Zanoni, R. — AF8, HI11
Zaremba, E. — AH8
Zarestky, J.L. — BK18, KP12
Zasadzinski, J.A. — KQ10
Zasadzinski, J.A.N. — KQ1
Zasadzinski, J.F. — AP5, DO11, DO14, EO12, GO14
Zayhowski, J.J. — KS13
Zdetsis, A.D. — NF8, NL8
Zegenhagen, J. — DI10
Zehner, D.M. — EJ3, EV7, HJ2, HJ3
Zeigler, J. — GS6
Zelaya-Angel, O. — AI7
Zeller, H.R. — KI12, KI13
Zeller, R. — KH2
Zengju, Tian — EK4
Zerbi, G. — DL14, EX3, EX9, JW9
Zettl, A. — BO11, DM12, DM13, DM14, GM11, GM12
Zhang, A. — HWb6
Zhang, C. — NJ12
Zhang, C.H. — GU8, GU9, GU10
Zhang, Chun-Si — DJ7, GJ9
Zhang, F.C. — AR9, DS6, JR1
Zhang, J. — Gwa24
Zhang, J.M. — NP2
Zhang, J.P. — EK3
Zhang, J.Q. — BS7
Zhang, K.J. — GP13
Zhang, L. — NN8
Zhang, Ming-Sheng — KR9, KR10
Zhang, S.B. — AS6
Zhang, S.L. — DT6
Zhang, Tao — BJ12
Zhang, X.C. — BJ11
Zhang, X.G. — JK4
Zhang, X.J. — DM4
Zhang, Y.-C. — DH11
Zhang, Y.D. — BN9, BN10
Zhang, Y.Z. — ML4
Zhang, Z.Q. — EN9
Zhang, Z.-y. — KK12
Zhao, J. — KN2, KO6
Zhao, Qin — KL6
Zhao, Y.Z. — JV11
Zhao, Z. — BN6, HN7
Zhao, Z.X. — GP11, MR2, MR7
Zheng, H.Z. — KL10
Zheng, Y.D. — HS11
Zhong, F. — BM13
Zhou, D. — HM10, HM11
Zhou, D.-M. — MJ1
Zhou, H. — GP4
Zhou, H.X. — EP7
Zhou, J.B. — HR1
Zhou, L.W. — DR18
Zhou, T. — DN9
Zhou, Y.-H. — EP1, EP2, EP3
Zhou, Zi-fang — NM7
Zhu, Xiaodong — NE12
Zimm, Bruno H. — HC1
Zimmerman, Dan S. — EQ14
Zimmerman, G. O. — MP14
Zimmerman, G.O. — HV1, MP13
Zinn, W. — DP2
Zipperian, T.E. — ET7, ET10
Zochowski, S.W. — EQ11
Zoller, P. — EN12
Zucker, J.E. — GT7, MU1
Zuhr, R.A. — DI9
Zuleeg, R. — NS12
Zunger, Alex — BT10, BU17, ET5, EV3, HT7, JU13, JU14, JU15, JU16
Zuo, F. — AL17
Zwartz, E.G. — NN1